

Backscatter Sensors Communication for 6G Low-powered NOMA-enabled IoT Networks under Imperfect SIC

Manzoor Ahmed, Wali Ullah Khan, Asim Ihsan, Xingwang Li, Jianbo Li, and Theodoros A. Tsiftsis

Abstract—The combination of non-orthogonal multiple access (NOMA) using power-domain with backscatter sensor communication (BSC) is expected to connect a large-scale Internet of things (IoT) devices in future sixth-generation (6G) era. In this paper, we introduce a BSC in multi-cell IoT network, where a source in each cell transmits superimposed signal to its associated IoT devices using NOMA. The backscatter sensor tag (BST) also transmit data towards IoT devices by reflecting and modulating the superimposed signal of the source. A new optimization framework is provided that simultaneously optimizes the total power of each source, power allocation coefficient of IoT devices and reflection coefficient of BST under imperfect successive interference cancellation decoding. The objective of this work is to maximize the total energy efficiency of IoT network subject to quality of services of each IoT device. The problem is first transformed using the Dinkelbach method and then decoupled into two subproblems. The Karush-Kuhn-Tucker conditions and Lagrangian dual method are employed to obtain the efficient solutions. In addition, we also present the conventional NOMA network without BSC as a benchmark framework. Simulation results unveil the advantage of our considered NOMA BSC networks over the conventional NOMA network.

Index Terms—Sixth-generation (6G), backscatter sensor communication (BSC), energy efficiency, Internet of things (IoT), non-orthogonal multiple access (NOMA).

I. INTRODUCTION

In the last couple of years, Internet-of-things (IoT) has been emerged as a new technological innovation in a wide range of applications such as smart factories, smart cities, smart homes, smart hospitals, autonomous vehicles, and so on [1], [2]. The IoT is expected to connect billions of sensor devices in the future sixth-generation (6G) systems [3], which would require the efficient utilization of existing spectrum resources [4], [5]. However, one of the key challenges would be energy issues especially for those systems where the battery replacement of sensor devices can be very costly [6]. In particular, the sensor devices which are hidden in walls and appliances or deployed in radioactive areas and pressurized pipes, making battery replacement difficult if not possible [7]. In such circumstances, ambient energy harvesting is a highly desirable

approach to maintain the life of sensor devices for a long period [8], [9]. It is important to mention here that ambient energy can sufficiently power sensor devices due to their low energy consumption. In this regard, a promising solution is Backscatter communication (BC) [10]. BC allows the sensor devices to transmit data by reflecting and modulating the existed radio frequency signal [11].

A. Technical Literature Review

Recently, power-domain non-orthogonal multiple access (NOMA) has gained significant importance due to its high spectral efficiency and massive connectivity [12], [13]. Compared to orthogonal multiple access (OMA) techniques, NOMA supports multiple IoT devices over the same spectrum/time resources which can be accomplished through two techniques, i.e., superposition coding at transmitter side and successive interference cancellation (SIC) at receiving side [14], [15]. Various research works on backscatter communication in traditional OMA networks have been studied in literature. For example, Guo *et al.* [16] have provided the efficient power allocation approach for cooperative BC to investigate the achievable rate of the system. The authors of [17] computed a closed-form solution for the outage probability (OP) of BC. In [18], the authors derived a closed-form expression for the OP of a BC system over Rayleigh fading channels. They also investigated the trade-off between harvested energy and data rate through power splitting factor. Qian *et al.* [19] calculated a closed-form expression for the symbol-error rate and designed an efficient multi-level energy detector for BC system. The authors of [20] investigated an optimization problem for throughput maximization of BC through calculating the optimal reflection coefficient (RC) and the trade-off between active and sleep state. Jameel *et al.* [21] exploited Q-learning approach to improve the achievable data rate while the constraint on delay is taken into account. In addition, Li *et al.* [22] investigated security and reliability of BC by through calculating the OP and intercept probability (IP) of the system. Recently, the performance of BC has been investigated using reinforcement learning techniques. The authors of [23], [24] have provided intelligent power allocation algorithms to improve the performance of BC systems.

The integration of BC in NOMA has recently been studied in literature. For example, in [25], the expression of OP has been derived in NOMA BC network where a source is equipped with multi-antenna scenario. Zhang *et al.* [26] have derived a closed-form expression for the OP and ergodic capacity in NOMA BC symbiotic radio systems. The work of [27] has studied the security issues of NOMA BC network. Khan *et al.* [28] have considered NOMA BC in vehicle-to-everything network to maximize the sum capacity of the

Manzoor Ahmed and J. Li are with the College of Computer Science and Technology, Qingdao University, Qingdao 266071, China. (emails: manzoor.achakzai@gmail.com, lijianbo@qdu.edu.cn).

Wali Ullah Khan is with the Interdisciplinary Centre for Security, Reliability and Trust (SnT), University of Luxembourg, 1855 Luxembourg City, Luxembourg (Emails: waliullah.khan@uni.lu, waliullahkhan30@gmail.com).

Asim Ihsan is with the Department of Information and Communication Engineering, Shanghai Jiao Tong University, Shanghai 200240, China. (email: ihsanasim@sjtu.edu.cn). Xingwang Li is with the School of Physics and Electronic Information Engineering, Henan Polytechnic University, Jiaozuo, China (email: lixingwangbupt@gmail.com).

Theodoros A. Tsiftsis is with School of Electrical and Information Engineering, Jinan University, Zhuhai 519070, China (email: theodoros.tsiftsis@gmail.com).

system. To improve the spectrum management and network capacity, Liao *et al.* [29] have studied resource allocation problem in full duplex NOMA BC networks. The work of [30] has improved the average successful decoding bit by efficient RC selection criteria in NOMA BC network. In similar study, Farajzadeh *et al.* [31] have optimized unmanned aerial vehicle altitude and maximize the successful decoded bit rate of NOMA BC network. Yang *et al.* [32] have optimized the time and RC of BC to maximize the system minimum throughput. Moreover, the work of [33] has investigated the OP and the throughput of NOMA BC system. Besides, Li *et al.* [34] have studied the physical layer security of multiple-input single-output NOMA BC network. In [35], the authors have proposed an optimization problem of transmit power and RC for BC to maximize the energy efficiency (EE) of the system. To investigate the security and reliability of NOMA BC system, the authors of [36] have investigated the OP and IP under channel estimation error, imperfect SIC and residual hardware impairment. In addition, the joint optimization of power and RC under imperfect SIC was solved in [37] to maximize the sum rate of NOMA BC system.

B. Motivation and Contributions

The above-existed literature [16]–[35] considers perfect SIC at the receiver side which is impractical in real systems. Of course, a decoding error can occur during the SIC process at receiver side such that the interference of other devices cannot be removed. This will result in significant degradation of the system performance. Besides that, most of the research works consider only single-cell and two-user scenarios. Generally, a network consists of different cells having various sizes. These cells normally share the same spectrum resources to enhance the spectral efficiency, result in causing inter-cell interference to each other. Moreover, the works in [36], [37] consider imperfect SIC in the single-cell system but their objectives were to improve the sum-capacity and physical layer security. Based on the above observations, there is a need to investigate a system performance with multi-cell, considering inter-cell interference and imperfect SIC decoding. Thus, the problem that jointly optimizes the total power budget of source, power allocation coefficient (PAC) of IoT devices, and RC of backscatter tag in each cell to investigate the EE of NOMA BC in multi-cell network under imperfect SIC has not yet been investigated, to the best of our knowledge. To bridge this gap, this work aims at proposing a new optimization approach for maximizing the system EE of the multi-cell NOMA backscatter sensors communication (BSC) network under imperfect SIC decoding. Dinkelback method is first adopted to convert the objective of EE from the fractional form into a subtractive form. The converted problem is divided into subproblems and closed-form solutions are then derived based on dual method and Karush-Kuhn-Tucker (KKT) conditions. Simulation results show the benefit of our multi-cell NOMA BSC scheme compared to the benchmark multi-cell NOMA scheme in terms of system total EE. The main contributions of this paper are summarized as follow:

- 1) A new optimization framework for a multi-cell IoT network is considered, where a source in each cell transmits

a superimposed signal to its serving IoT devices using NOMA protocol. A backscatter sensor tag (BST) in each cell also transmits data symbols towards nearby IoT devices by reflecting and modulating the superimposed signal of the source node. The objective is to maximize the total achievable EE of BSC network under im-SIC decoding. We simultaneously optimize the RC of BST, PAC of IoT devices, and total power budget of the source in each cell subject to the quality of services of IoT devices.

- 2) The optimization problem to maximize the total EE is formulated as a non-convex which is very complex and hard to be solved. Hence, the Dinkelback method is first adopted to the original problem to convert the objective of EE from the fractional form into a subtractive form. The converted problem is then divided into two subproblems, i.e., power optimization at source and RC at BST in each cell. Next, we prove the RC subproblem as concave and exploit KKT conditions to obtain an efficient solution. Similarly, we prove that the power allocation subproblem is concave and solve it using the Lagrangian dual method.
- 3) We also investigate the same model without BSC (also known as pure NOMA IoT network without backscattering) and set it as the benchmark framework. The numerical results for the proposed framework are corroborated by using Monte Carlo simulation which demonstrates the advantage of NOMA BSC network over the conventional NOMA IoT network without BSC. In addition, the proposed algorithm is less complex and converges after few iterations.

The remaining of this paper is structured as follows: The system model and problem formulation are provided in Section II. The EE maximization solution is proposed in Section III. Simulation results and discussion is presented in Section IV followed by the concluding remarks in Section V.

II. SYSTEM MODEL AND PROBLEM FORMULATION

We consider a multi-cell BSC network as shown in Fig. 1, wherein each cell, a source (denoted as \mathcal{S}) communicates with two downlink IoT devices ($\mathcal{D}_{i,k}$ and $\mathcal{D}_{j,k}$) using NOMA protocol¹. The network also consists of F uplink BSTs where its set can be denoted as $f = \{1, 2, 3, \dots, F\}$. A BST in each cell also receives the downlink superimposed signal from \mathcal{S} , uses it to modulate information, and then reflects it towards IoT devices in the uplink direction, where the IoT devices also act as readers. The set of cells can be denoted as K such as $k = \{1, 2, 3, \dots, K\}$, where k represents source \mathcal{S}_k . We assume that: 1) All the transmitters and receivers are using single antenna for communication; 2) all the sources reuse the same spectrum/time resources; 3) the channel state information of IoT devices in each cell is available at the source [39]; 4) a decoding error can occur during the SIC process at receiver

¹This work considers two IoT devices in each cell, however, it can be easily extended to the multi-user scenario. For instance, if the region of each cell is partitioned into multiple clusters and each cluster consists of two IoT devices. In such a case, NOMA is among IoT devices in the same cluster and OMA can be utilized between different clusters [38].

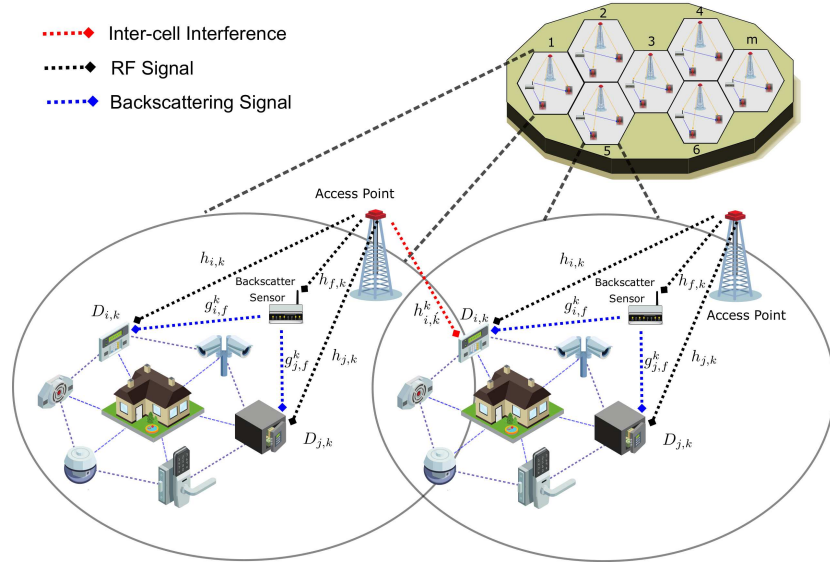


Fig. 1: Illustration of system model.

side such that the interference of other devices cannot be removed. Therefore, we consider SIC with decoding error. A superimposed signal x_k transmitted by source S_k to $\mathcal{D}_{i,k}$ and $\mathcal{D}_{j,k}$ can be expressed as:

$$x_k = \sqrt{P_k A_{i,k}} x_{i,k} + \sqrt{P_k A_{j,k}} x_{j,k}, \quad (1)$$

where P_k is the transmit power of S_k , $A_{i,k}$ and $A_{j,k}$ denote the PAC of S_k . $x_{i,k}$ and $x_{j,k}$ are the unit power data symbols of $\mathcal{D}_{i,k}$ and $\mathcal{D}_{j,k}$ from S_k . Meanwhile, the BST denoted as $\mathcal{B}_{f,k}$ also receives x_k from S_k , reflect it towards $\mathcal{D}_{i,k}$ and $\mathcal{D}_{j,k}$ by adding data symbol $w(t)$ such that $\mathbb{E}[|w(t)|^2] = 1$, where $\mathbb{E}[\cdot]$ represents the expectation operation. Therefore, $\mathcal{D}_{i,k}$ and $\mathcal{D}_{j,k}$ receive signals from both S_k and $\mathcal{B}_{f,k}$. Following the work in [40], If the channel from S_k to $\mathcal{D}_{i,k}$ and $\mathcal{D}_{j,k}$ is modeled as $h_{i,k} = \bar{h}_{i,k} d_{i,k}^{-\rho/2}$ and $h_{j,k} = \bar{h}_{j,k} d_{j,k}^{-\rho/2}$, where $\bar{h}_{\varsigma,k} \sim \mathcal{CN}(0, 1)$, $\varsigma \in \{i, j\}$ are the coefficient of Rayleigh fading, $d_{\varsigma,k}$ is the distance from S_k to $\mathcal{D}_{i,k}$ and $\mathcal{D}_{j,k}$ and ρ shoes the path loss exponent. Then, the received signal of $\mathcal{D}_{i,k}$ and $\mathcal{D}_{j,k}$ can be written as:

$$y_{i,k} = \sqrt{h_{i,k}} x_k + \sqrt{\Phi_{f,k} g_{i,f}^k} (h_{f,k} x_k) w(t) + \sum_{k'=1, k' \neq k}^K \sqrt{P_{k'} h_{i,k'}^k} x_{k'} + \varpi_{i,k}, \quad (2)$$

$$y_{j,k} = \sqrt{h_{j,k}} x_k + \sqrt{\Phi_{f,k} g_{j,f}^k} (h_{f,k} x_k) w(t) + \sum_{k'=1, k' \neq k}^K \sqrt{P_{k'} h_{j,k'}^k} x_{k'} + \varpi_{j,k}, \quad (3)$$

where in both (2) and (3), the first segment refer to the desired signal of S_k , the second segment is the reflected signal of $\mathcal{B}_{f,k}$ and the third segment represents the inter-cell interference of neighboring cells. Further, $h_{f,k}$ is the channel gain between $\mathcal{B}_{f,k}$ and S_k , $\Phi_{f,k}$ refers to the RC of $\mathcal{B}_{f,k}$. Further, $g_{i,f}^k$ and $g_{j,f}^k$ denote the channel gains from $\mathcal{B}_{f,k}$ to $\mathcal{D}_{i,k}$ and $\mathcal{D}_{j,k}$. In

addition, $P_{k'}$ is the interference power from $S_{k'}$, $h_{i,k'}^k$ and $h_{j,k'}^k$ are the channel gains from $S_{k'}$ to $\mathcal{D}_{i,k}$ and $\mathcal{D}_{j,k}$. Moreover, $\varpi_{i,k}$ and $\varpi_{j,k}$ are the additive white Gaussian noises (AWGN) with zero mean and σ^2 variance. According to the NOMA, $\mathcal{D}_{i,k}$ can decodes the signals $x_{i,k}$ and $w(t)$ by applying the SIC technique. In contrary, $\mathcal{D}_{j,k}$ cannot apply SIC and decodes the signal $x_{j,k}$ with interference.

By considering the detecting and decoding sensitivity of receiver, $\mathcal{B}_{f,k}$ a decoding error can occur during the SIC process at $\mathcal{D}_{i,k}$ such that the interference of $\mathcal{D}_{j,k}$ cannot be removed. Therefore, the received signal to interference plus noise ratio (SINR) of $\mathcal{D}_{i,k}$ when subtracting the signal of $\mathcal{D}_{j,k}$ can be given as:

$$\gamma_{i \rightarrow j}^k = \frac{P_k A_{j,k} |h_{i,k}|^2 + \Phi_{f,k} |h_{f,k}|^2 |g_{i,f}^k|^2}{P_k A_{i,k} (|h_{i,k}|^2 + \Phi_{f,k} |h_{f,k}|^2 |g_{i,f}^k|^2) + \Delta_{j,k'}^k + \sigma^2}, \quad (4)$$

where $\Delta_{j,k'}^k = |h_{j,k'}^k|^2 \sum_{k'=1}^K P_{k'}$ is the inter-cell interference due to the co-channel deployment. The SINR at $\mathcal{D}_{i,k}$ to decode its own signal can be stated as:

$$\gamma_{i \rightarrow i}^k = \frac{P_k A_{i,k} (|h_{i,k}|^2 + \Phi_{f,k} G_{i,k})}{P_k A_{j,k} |h_{i,k}|^2 \beta + \Delta_{i,k'}^k + \sigma^2}, \quad (5)$$

where $G_{i,k} = |h_{f,k}|^2 |g_{i,f}^k|^2$. β represents the imperfect SIC parameter which is given as $\beta = \mathbb{E}[|x_{i,k} - \tilde{x}_{i,k}|^2]$, where $x_{i,k} - \tilde{x}_{i,k}$ stands for the difference between the original and the estimated signals. The corresponding rate of $\mathcal{D}_{i,k}$ can be written as $R_{i,k} = \log_2(1 + \gamma_{i \rightarrow i}^k)$. The SINR at $\mathcal{D}_{j,k}$ to decode $x_{j,k}$ can be written as:

$$\gamma_{j \rightarrow j}^k = \frac{P_k A_{j,k} (|h_{j,k}|^2 + \Phi_{f,k} G_{j,k})}{P_k A_{i,k} (|h_{j,k}|^2 + \Phi_{f,k} G_{j,k}) + \Delta_{j,k'}^k + \sigma^2}, \quad (6)$$

where $G_{j,k} = |h_{f,k}|^2 |g_{j,f}^k|^2$. Thus, its corresponding data rate is can be written as $R_{j,k} = \log_2(1 + \gamma_{j \rightarrow j}^k)$.

The objective of this work is to maximize the total EE of

multi-cell NOMA BSC network. The total EE is given by

$$EE = \sum_{k=1}^K \left(\frac{R_k}{P_k \Lambda_{i,k} + P_k \Lambda_{j,k} + p_c} \right), \quad (7)$$

where $R_k = R_{i,k} + R_{j,k}$ is the sum rate of \mathcal{S}_k while the circuit power is represented by p_c . The EE of the system can be maximized through the efficient allocation of transmit power of \mathcal{S}_k , PAC of IoT devices, and the RC of BST in each cell. In addition, we also aim to ensure the minimum data rate of IoT devices in each cell. Mathematically, a joint optimization problem (P) is to maximize the total EE of multi-cell NOMA BSC network can be formulated as:

$$(P) \quad \max_{(\Lambda_{i,k}, \Lambda_{j,k}, \Phi_{f,k})} EE \quad (8)$$

$$\begin{aligned} \text{s.t. } C1: & P_k \Lambda_{i,k} (|h_{i,k}|^2 + \Phi_{f,k} G_{i,k}) \geq (2^{R_{min}} - 1) \\ & \times (|h_{i,k}|^2 P_k \Lambda_{j,k} \beta + \Delta_{i,k'}^k + \sigma^2), \forall k, \\ C2: & P_k \Lambda_{j,k} (|h_{j,k}|^2 + \Phi_{f,k} G_{j,k}) \geq (2^{R_{min}} - 1) \\ & \times (P_k \Lambda_{i,k} (|h_{j,k}|^2 + \Phi_{f,k} |G_{j,k}|) + \Delta_{j,k'}^k + \sigma^2), \forall k, \\ C3: & P_k \Lambda_{i,k} \leq P_k \Lambda_{j,k}, \forall k, \forall i, j, \\ C4: & 0 \leq P_k \leq P_{max}, \forall k, \\ C5: & \Lambda_{i,k} + \Lambda_{j,k} \leq 1, \forall k, \\ C6: & 0 \leq \Phi_{f,k} \leq 1, \forall f, \forall k, \end{aligned}$$

where constraints C1 and C2 guarantee the minimum data rate of IoT $\mathcal{D}_{i,k}$ and $\mathcal{D}_{j,k}$ associated with \mathcal{S}_k . Constraint C3 ensures the SIC decoding at receivers. Constraint C4 limits the transmit power of \mathcal{S}_k . Constraint C5 describes the condition for PAC of IoT devices connected to \mathcal{S}_k while constraint C6 limits the RC of BST between 0 and 1.

III. ENERGY EFFICIENCY MAXIMIZATION SOLUTION

The above EE maximization problem defined in (8) is coupled on two variables in each cell, i.e., 1) Transmit power of the source and PAC of IoT devices in each cell, and 2) RC of BST in each cell. Thus, it is very hard to solve it directly. Therefore, this problem can be solved in three steps: i) First, we apply Dinkelbach method to transform the objective function of (P) into subtractive one; ii) second, on the fixed value of source transmit power in each cell, we compute the efficient RC of BST in each cell, and iii) third, we substitute the RC of BST in (8) and calculate the transmit power of source and PAC of IoT devices. Based on Dinkelbach method, the problem in (8) can be transformed as:

$$\begin{aligned} & \max_{(\Lambda_{i,k}, \Lambda_{j,k}, \Phi_{f,k})} \sum_{k=1}^K R_k - \Pi \sum_{k=1}^K P_k (\Lambda_{i,k} + \Lambda_{j,k}) + p_c, \\ \text{s.t. } & C1 - C6, \end{aligned} \quad (9)$$

where Π shows the maximum EE and it can be achieved when

$$\sum_{k=1}^K R_k - \Pi^* \left(\sum_{k=1}^K P_k (\Lambda_{i,k}^* + \Lambda_{j,k}^*) + p_c \right) = 0. \quad (10)$$

The problem in (9) is still hard to be solved due to the interference terms in the SINR of $\mathcal{D}_{i,k}$ and $\mathcal{D}_{j,k}$ and the coupled variables Λ_k and $\Phi_{f,k}$. Thus, we decouple problem

(9) into two subproblems, i.e., RC selection subproblem and transmit power allocation subproblem.

A. Efficient Reflection Coefficient Selection

Here we compute the efficient RC of BST in each cell. For any given power allocation Λ_k^* at \mathcal{S}_k in each cell, the optimization problem in (9) can be simplified to BST RC selection subproblem as:

$$\begin{aligned} & \max_{(\Phi_{f,k})} \sum_{k=1}^K \log_2 \left\{ \left(1 + \frac{X_{i,k} + \Phi_{f,k} Y_{i,k}}{Z_{i,k}} \right) \right. \\ & \left. + \log_2 \left(1 + \frac{X_{j,k} + \Phi_{f,k} Y_{j,k}}{Z_{j,k} + \Phi_{f,k} W_{j,k}} \right) \right\} \\ & - \Pi \sum_{k=1}^K P_k (\Lambda_{i,k}^* + \Lambda_{j,k}^*) + p_c, \end{aligned} \quad (11)$$

$$\text{s.t. } C1, C2, C4, C6,$$

where $X_{i,k} = P_k \Lambda_{i,k}^* |h_{i,k}|^2$, $Y_{i,k} = P_k \Lambda_{i,k}^* G_{i,k}$, $Z_{i,k} = P_k \Lambda_{j,k}^* |h_{i,k}|^2 \beta + \Delta_{i,k'}^k + \sigma^2$, $X_{j,k} = P_k \Lambda_{j,k}^* |h_{j,k}|^2$, $Y_{j,k} = P_k \Lambda_{j,k}^* G_{j,k}$, $Z_{j,k} = P_k \Lambda_{i,k}^* |h_{j,k}|^2 \beta + \Delta_{j,k'}^k + \sigma^2$ and $W_{j,k} = P_k \Lambda_{i,k}^* G_{j,k}$. By using the following proposition, we demonstrate that R_k is a concave/convex using $\Phi_{f,k}$.

Proposition 1. *The sum rate of \mathcal{S}_k*

$$\begin{aligned} R_k = \log_2 \left\{ \left(1 + \frac{X_{i,k} + \Phi_{f,k} Y_{i,k}}{Z_{i,k}} \right) \right. \\ \left. + \log_2 \left(1 + \frac{X_{j,k} + \Phi_{f,k} Y_{j,k}}{Z_{j,k} + \Phi_{f,k} W_{j,k}} \right) \right\}, \end{aligned} \quad (12)$$

is concave/convex with reference to $\Phi_{f,k}$.

Proof. Refer to Appendix A. \square

According to the Proposition 1, the optimization problem (11) is concave which motivates us to exploit KKT conditions for obtaining optimal $\Phi_{f,k}$.

Proposition 2. *The closed-form of BST RC can be then expressed as:*

$$\Phi_{f,k} = \left[\frac{(2^{\gamma_{i,k}^{min}} - 1) - X_{i,k}}{Y_{i,k}} \right], \quad (13)$$

Proof. Please, refer to Appendix B. \square

In the sequel, we calculate efficient power allocation in each cell.

B. Efficient Power Allocation

Here we calculate the efficient transmit power of source and PAC of IoT devices in each cell. For the fixed value of BST RC $\Phi_{f,k}^*$, the optimization problem in (9) can be then written as:

$$\begin{aligned} & \max_{(\Lambda_{i,k}, \Lambda_{j,k})} \sum_{k=1}^K E_k = \max_{(\Lambda_{i,k}, \Lambda_{j,k})} \sum_{k=1}^K \frac{R_{i,k} + R_{j,k}}{P_k (\Lambda_{i,k} + \Lambda_{j,k}) + p_c} \\ \text{s.t. } & C1 - C5. \end{aligned} \quad (14)$$

We can also write Equation (5) and (6) as:

$$\gamma_{i \rightarrow i}^k = \frac{P_k A_{i,k} A_{i,k}}{P_k A_{j,k} B_{i,k} + C_{i,k}}, \quad (15)$$

with $A_{i,k} = |h_{i,k}|^2 + \Phi_{f,k} G_{i,k}$, $B_{i,k} = |h_{i,k}|^2 \beta$, $C_{i,k} = \Delta_{i,k'}^k + \sigma^2$, and

$$\gamma_{j \rightarrow j}^k = \frac{P_k A_{j,k} A_{j,k}}{P_k A_{i,k} B_{j,k} + C_{j,k}}, \quad (16)$$

where $A_{j,k} = |h_{j,k}|^2 + \Phi_{f,k} G_{j,k}$, $B_{j,k} = |h_{j,k}|^2 + \Phi_{f,k} G_{j,k}$, $C_{j,k} = \Delta_{j,k'}^k + \sigma^2$. In the following proposition, we will prove that (14) is concave/convex regarding $\mathbf{A}_k = \{A_{i,k}, A_{j,k}\}$.

Proposition 3. *The sum rate of \mathcal{S}_k*

$$R_k = \log_2 \left(1 + \frac{P_k A_{i,k} A_{i,k}}{P_k A_{j,k} B_{i,k} + C_{i,k}} \right) + \log_2 \left(1 + \frac{P_k A_{j,k} A_{j,k}}{P_k A_{i,k} B_{j,k} + C_{j,k}} \right) \quad (17)$$

is concave/convex with reference to $\mathbf{A}_k = \{A_{i,k}, A_{j,k}\}$.

Proof. The proof is demonstrate in Appendix C. \square

Based on Proposition 3, the objective function in (14) is concave-convex fractional programming problem, which can be solved through Dinkelbach algorithm as follow:

$$\begin{aligned} \max_{(A_{i,k}, A_{j,k})} \sum_{k=1}^K E_k &= \max_{(A_{i,k}, A_{j,k})} \sum_{k=1}^K F(\Pi) \\ &= \max_{(A_{i,k}, A_{j,k})} \sum_{k=1}^K R_k - \Pi \left(\sum_{k=1}^K P_k (A_{i,k} + A_{j,k}) - p_c \right) \quad (18) \end{aligned}$$

s.t. C1 – C5.

where $\Pi = \frac{R_k}{\sum_{k=1}^K P_k (A_{i,k} + A_{j,k}) + p_c}$, while $F(\Pi)$ is the parametric form of fractional objective function in (18). Solving the roots of $F(\Pi)$ is equivalent to computing the fractional objective function in (18). $F(\Pi)$ as function of Π is convex because it is negative when Π tends to infinity and is positive when Π approaches minus infinity. Therefore, motivated by the above observations, this convex problem can be solved through Lagrangian dual decomposition method. The Lagrangian function of problem (18) can be defined as:

$$\begin{aligned} L(\mathbf{A}_k, \boldsymbol{\lambda}_k, \mu_k, \epsilon_k) &= \sum_{k=1}^K \left\{ \log_2 \left(1 + \frac{P_k A_{i,k} A_{i,k}}{P_k A_{j,k} B_{i,k} + C_{i,k}} \right) \right. \\ &\quad \left. + \log_2 \left(1 + \frac{P_k A_{j,k} A_{j,k}}{P_k A_{i,k} B_{j,k} + C_{j,k}} \right) \right\} \\ &\quad - \Pi \sum_{k=1}^K P_k (A_{i,k} + A_{j,k}) - p_c + \lambda_{i,k} (P_k A_{i,k} A_{i,k} \\ &\quad - (2^{R_{min}} - 1) P_k A_{j,k} B_{i,k} + C_{i,k}) + \lambda_{j,k} (P_k A_{j,k} A_{j,k} \\ &\quad - (2^{R_{min}} - 1) (P_k A_{i,k} B_{j,k} + C_{j,k})) + \mu_k (P_{max} - P_k) \\ &\quad + \epsilon_k (1 - A_{i,k} - A_{j,k}), \quad (19) \end{aligned}$$

where $\boldsymbol{\lambda}_k = \{\lambda_{i,k}, \lambda_{j,k}\}$, μ_k , and ϵ_k are the dual variables, which are related to the constraints C1, C2, C4, and C5. The

Lagrangian dual function can be presented as:

$$g(\boldsymbol{\lambda}_k, \mu_k, \epsilon_k) = \max_{\mathbf{A}_k > 0, \boldsymbol{\lambda}_k, \mu_k, \epsilon_k \geq 0} L(\mathbf{A}_k, \boldsymbol{\lambda}_k, \mu_k, \epsilon_k) \quad (20)$$

Then, its a dual problem can be formulated as follow:

$$\min_{\boldsymbol{\lambda}_k, \mu_k, \epsilon_k \geq 0} g(\boldsymbol{\lambda}_k, \mu_k, \epsilon_k) \quad (21)$$

For the fixed dual variables and given EE Π , the formulated optimization problem depends on KKT conditions.

Proposition 4. *The closed-form expression for energy-efficient PAC of $\mathcal{D}_{i,k}$ and $\mathcal{D}_{j,k}$ can be derived as:*

$$A_{i,k}^* = \left[\frac{-b \pm \sqrt{b^2 - 4ac}}{2a} \right]^+ \quad (22)$$

$$A_{j,k}^* = 1 - A_{i,k}^* \quad (23)$$

where $[\cdot]^+ = \max[0, \cdot]$ and the values of

$$a = P_k^2 (-A_{i,k} A_{j,k} B_{j,k} (1 + \lambda_{i,k}) (C_{i,k} + B_{i,k} P_k) + A_{i,k} B_{j,k}^2 (1 + \lambda_{i,k}) (C_{i,k} + B_{i,k} P_k) + A_{i,k} A_{j,k} B_{i,k} (1 + \lambda_{j,k}) (C_{j,k} + B_{j,k} P_k) - A_{j,k} B_{i,k}^2 (1 + \lambda_{j,k}) (C_{j,k} + B_{j,k} P_k)), \quad (24)$$

$$b = P_k (C_{i,k} + B_{i,k} P_k) (-A_{i,k} C_{j,k} (-2B_{j,k} (1 + \lambda_{i,k}) + A_{j,k} (2 + L_{i,k} + \lambda_{j,k})) + A_{i,k} A_{j,k} B_{j,k} (\lambda_{i,k} - \lambda_{j,k}) P_k + 2A_{j,k} B_{i,k} (1 + \lambda_{j,k}) (C_{j,k} + B_{j,k} P_k)), \quad (25)$$

$$c = (C_{i,k} + B_{i,k} P_k) (A_{i,k} C_{j,k}^2 (1 + \lambda_{i,k}) + A_{j,k} (-C_{i,k} (1 + \lambda_{j,k}) (C_{j,k} + B_{j,k} P_k) + P_k (A_{i,k} C_{j,k} (1 + \lambda_{i,k}) - B_{i,k} (1 + \lambda_{i,k}) (C_{j,k} + B_{j,k} P_k))). \quad (26)$$

Proof. Please, refer to Appendix D. \square

Next we calculate the optimal transmit power of each source, i.e., P_k . To do so, we differentiate (19) with respect to P_k , it results as:

$$\tau + \chi P_k + \psi P_k^2 + \Gamma P_k^3 + \omega P_k^4 = 0, \quad (27)$$

where τ, χ, ψ, Γ and ω are given in (26)-(29) on the top of the next page. Equation (27) is the polynomial of order four which can be easily solved by any conventional solver. The objective of the problem is to maximize the EE, thus, P_k^* can be founded through the larger root of (27). With optimal $A_{i,k}^*$, $A_{j,k}^*$ and P_k^* , problem (20) can be written as:

$$\begin{aligned} \max_{(A_{i,k}^*, A_{j,k}^*, P_k^*)} \sum_{k=1}^K \left\{ \log_2 \left(1 + \frac{P_k^* A_{i,k}^* A_{i,k}^*}{P_k^* A_{j,k}^* B_{i,k} + C_{i,k}} \right) \right. \\ \left. + \log_2 \left(1 + \frac{P_k^* A_{j,k}^* A_{j,k}^*}{P_k^* A_{i,k}^* B_{j,k} + C_{j,k}} \right) \right\} \\ - \Pi \sum_{k=1}^K P_k^* (A_{i,k}^* + A_{j,k}^*) + p_c, \quad (33) \end{aligned}$$

subject to: $\boldsymbol{\lambda}_k, \epsilon_k \geq 0$

Subsequently, we use sub-gradient method to iteratively update the Lagrangian multipliers $\lambda_{i,k}$, $\lambda_{j,k}$, μ_k and ϵ_k as [41]:

$$\begin{aligned} \lambda_{i,k}(t+1) &= \lambda_{i,k}(t) + \delta(t) (P_k^* A_{i,k}^* A_{i,k}^* \\ &\quad - (2^{R_{min}} - 1) P_k^* A_{j,k}^* B_{i,k} + C_{i,k}), \forall k, \quad (34) \end{aligned}$$

$$\tau = C_{i,k}C_{j,k}(-A_{j,k}C_{i,k}(-1 + \Lambda_{i,k}))(1 + \lambda_{j,k}) + C_{j,k}(A_{i,k}\Lambda_{i,k}(1 + \lambda_{i,k}) - C_{i,k}(\mu_k + \Pi)), \quad (28)$$

$$\chi = C_{i,k}C_{j,k}(2(B_{i,k}C_{j,k}(-1 + \Lambda_{i,k}) - B_{j,k}C_{i,k}\Lambda_{i,k})(\mu_k + \Pi) + A_{j,k}(-1 + \Lambda_{i,k})(2B_{i,k}(-1 + \Lambda_{i,k})(1 + \lambda_{j,k}) - A_{i,k}\Lambda_{i,k}(2 + \lambda_{i,k} + \lambda_{j,k}) + C_{i,k}(\mu_k + \Pi)) + A_{i,k}\Lambda_{i,k}(2B_{j,k}\Lambda_{i,k}(1 + \lambda_{i,k}) - C_{j,k}(\mu_k + \Pi))), \quad (29)$$

$$\psi = -(B_{i,k}^2C_{j,k}^2(-1 + \Lambda_{i,k})^2 - 4B_{i,k}B_{j,k}C_{i,k}C_{j,k}(-1 + \Lambda_{i,k})\Lambda_{i,k} + B_{j,k}^2C_{i,k}^2\Lambda_{i,k}^2)(\mu_k + \Pi) + A_{i,k}\Lambda_{i,k}(B_{j,k}^2C_{i,k}\Lambda_{i,k}^2(1 + \lambda_{i,k}) + B_{i,k}C_{j,k}^2(-1 + \Lambda_{i,k})(\mu_k + \Pi) - 2B_{j,k}C_{i,k}C_{j,k}\Lambda_{i,k}(\mu_k + \Pi)) - A_{j,k}(-1 + \Lambda_{i,k})(B_{i,k}^2C_{j,k}(-1 + \Lambda_{i,k})^2(1 + \lambda_{j,k}) - B_{i,k}C_{j,k}(-1 + \Lambda_{i,k})(A_{i,k}\Lambda_{i,k}(1 + \lambda_{j,k}) - 2C_{i,k}(\mu_k + \Pi)) - C_{i,k}\Lambda_{i,k}(B_{j,k}C_{i,k}(\mu_k + \Pi) + A_{i,k}(-B_{j,k}\Lambda_{i,k}(1 + \lambda_{i,k}) + C_{j,k}(\mu_k + \Pi)))), \quad (30)$$

$$\Gamma = (B_{j,k}\Lambda_{i,k}(-2B_{i,k}^2C_{j,k}(-1 + \Lambda_{i,k})^2 + 2B_{i,k}(B_{j,k}C_{i,k} + A_{i,k}C_{j,k})(-1 + \Lambda_{i,k})\Lambda_{i,k} - A_{i,k}B_{j,k}C_{i,k}\Lambda_{i,k}^2) + A_{j,k}(-1 + \Lambda_{i,k})(B_{i,k}^2C_{j,k}(-1 + \Lambda_{i,k})^2 - B_{i,k}(2B_{j,k}C_{i,k} + A_{i,k}C_{j,k})(-1 + \Lambda_{i,k})\Lambda_{i,k} + A_{i,k}B_{j,k}C_{i,k}\Lambda_{i,k}^2))(\mu_k + \Pi), \quad (31)$$

$$\omega = -B_{i,k}B_{j,k}(-1 + \Lambda_{i,k})\Lambda_{i,k}(B_{i,k}(-1 + \Lambda_{i,k}) - A_{i,k}\Lambda_{i,k})(A_{j,k} - A_{j,k}\Lambda_{i,k} + B_{j,k}\Lambda_{i,k})(\mu_k + \Pi). \quad (32)$$

$$\lambda_{j,k}(t+1) = \lambda_{j,k}(t) + \delta(t)(P_k^*A_{j,k}^*A_{j,k} - (2^{R_{min}} - 1)(P_k^*A_{i,k}^*B_{j,k} + C_{j,k})), \forall k, \quad (35)$$

$$\epsilon_k(t+1) = \epsilon_k(t) + \delta(t)(1 - (A_{i,k}^* + A_{j,k}^*)), \forall k, \quad (36)$$

$$\mu_k(t+1) = \mu_k(t) + \delta(t)(P_{max} - P_k^*), \forall k, \quad (37)$$

where t is the index of iteration. Equations (34), (35), (36), and (37) are iteratively calculated until the required criterion satisfied.

C. Proposed Algorithm and Complexity Analyses

Here, we design algorithm based on the solutions provided in Section III-A and B, respectively. As shown in Algorithm 1, we initialize all the system parameters and variables. For the given values of P_k , $\Lambda_{i,k}$ and $\Lambda_{j,k}$, we compute $\Phi_{f,k}$. Subsequently, we substitute the value of $\Phi_{f,k}^*$ in power allocation subproblem (14) and calculate $\Lambda_{i,k}$ and $\Lambda_{j,k}$ followed by P_k . Then, we iteratively update $\lambda_{i,k}$, $\lambda_{j,k}$ and ϵ_k . The above process will continue until convergence criteria satisfied.

The computational complexity of the proposed optimization framework can be calculated regarding the number of iterations. The complexity of our algorithm depends on the different variables and parameters of the system such number of cells and the number of users, i.e., K, I, J . Based on these observation, the complexity of the proposed algorithm in any given iteration is computed as $\mathcal{O}[(I + J)K]$. Since we have considered two user in each cell, therefore, the computational complexity can also be written as $\mathcal{O}[2K]$. Further, if the number of total iteration required for convergence is T , the total computational complexity becomes $\mathcal{O}[2TK]$.

IV. NUMERICAL RESULTS AND DISCUSSION

In this section, we provide the simulation results to evaluate the performance of the proposed framework. Unless specified otherwise the system parameters are taken as follow: $\sigma=0.01$, $\beta=0.1$, $K=10$, $p_c=0.1$ W, and $P_{max}=32$ dBm. In the considered problem, the power allocation is always lower bounded by the R_{min} in order to make the impact of changing P_{max} more prominent. In the first three results of this section, we

Algorithm 1: Proposed resource optimization algorithm.

if $t = 0$ **then**

Initialize all parameters and variables, i.e., number of cells, number of users, number of BSTs, maximum power budget of each source, RC of each BST, variance, minimum data rate, circuit power, values of imperfect SIC and channel gains.

else

First we calculate the reflection coefficient of backscatter tag in each cell for the given values of $\Lambda_{i,k}, \Lambda_{i,k}$ and P_k

for $k = 1 : K$ **do**

| Find $\Phi_{f,k}$ according to (13)

end

Next we substitute the value of $\Phi_{f,k}^*$ in (14) and calculate the values of $\Lambda_{i,k}, \Lambda_{i,k}$ and P_k

while not converge do

| **for** $k = 1 : K, i = 1 : I, j = 1 : J$ **do**

| | Compute $\Lambda_{i,k}$ according to (22) and $\Lambda_{j,k}$ according to (23)

| | Compute P_k according to (27)

| | Update the dual variables $\lambda_{i,k}, \lambda_{j,k}$ and ϵ_k

| **end**

end

Return $P_k^*, \Lambda_{i,k}^*, \Lambda_{j,k}^*, \Phi_{f,k}$

end

have taken $R_{min}=0$. To analyze the benefits of backscattering, the performance of the proposed framework WBS (with backscatter sensor) is compared with a simplified network with no backscatter sensor (NBS)².

The effect of increasing P_{max} on the total EE of the system is presented in Fig. 2. An increase in the value of P_{max} results in increasing the EE of the system initially. However, after a certain point, an increase in P_{max} has no impact on the total EE. This is because, at these points, the transmission power

²Due to the novelty of the proposed framework, it is difficult to compare it with the existing works of the literature. Thus, we resort to compare it with pure NOMA without backscatter communication.

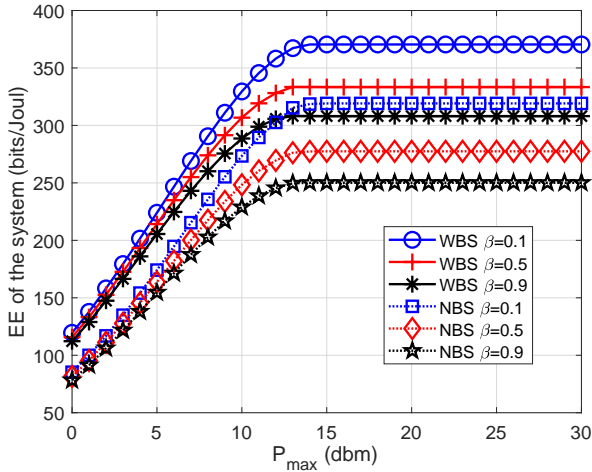


Fig. 2: The impact of increasing P_{max} on the total EE of the system with different values of β

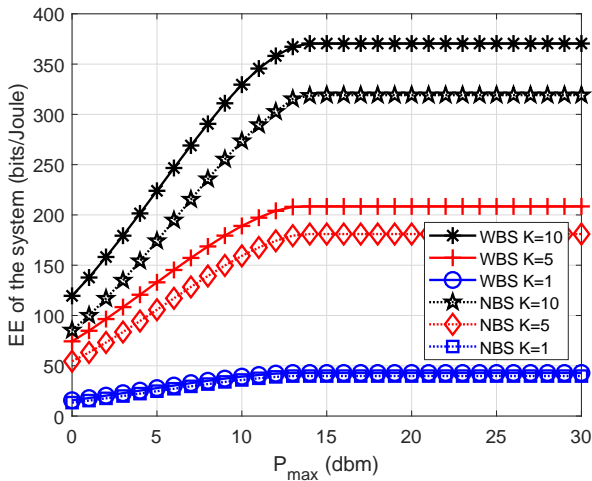


Fig. 3: The effect of increasing P_{max} on the total EE for different number of cell in the system

is efficient, and allocating more power for the transmission results in decreasing the total EE of the system. Thus, when the value of P_{max} is further increased, the allocated power for the transmission remains unchanged. Further, it can be seen that smaller values of β result in providing more EE. The reason is that, at small β , less interference is faced by the near IoT devices, whereas, increasing β would increase the SIC error resulting in the reduction of the overall system EE. At smaller values of P_{max} , the transmission power is also very less, this cause a very small interference to the other IoT devices in the system. Thus, the values of total EE for different β have a very small gap, for smaller values of P_{max} . However, this gap increases with the increasing P_{max} , i.e., as the transmission power increases the interference also increase and the impact of imperfect SIC on the EE becomes more prominent. It is clear from Fig. 2 that the system with BST outperforms the network with no BST for all values of P_{max} .

The total EE of the system also depends on total cells in the network. The impact of increasing P_{max} on the EE of system

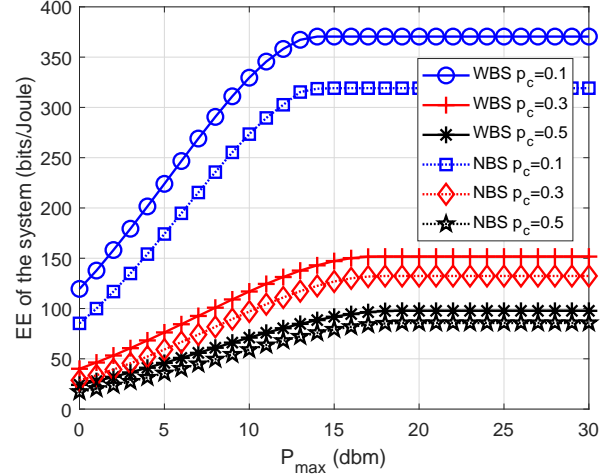


Fig. 4: The effect of increasing P_{max} on the EE for different p_c

containing different K is shown in the Fig. 3. For any value of K , increasing the value of P_{max} increases the EE initially, however the efficiency becomes constant after a certain point because the transmission power remains unchanged. It is interesting to see that the difference between the EE offered the WBS and NBS systems increases with increasing P_{max} . This is because when the transmission power increases, the interference faced by all the IoT devices also increase. In the case of WBS systems, the increased transmission power also results in increasing the BST rate. Hence, the increase in the EE of WBS is more, as compared to the NBS. With more number of K in the system, the benefit of BST becomes more clear, as it clear from the Fig. 3 that the gap between WBS and NBS increases with

The circuit power consumption (p_c) also affects the EE of the network. Fig. 4 shows that larger values of p_c decreases the EE of the system. Further, it is clear from the figure that the WBS systems outperform the NBS for all values of P_{max} . An important point to note in Fig. 4 is that, when p_c is increased the optimal value of power allocation is achieved at comparatively greater value of P_{max} . As in the case of $p_c=0.1$, the EE becomes constant at $P_{max}=16$ dBm. However, for $p_c=0.3$ and $p_c=0.5$, the convergence behavior of EE is observed for $P_{max} \geq 19$ and 21, respectively. This shows that for smaller values of p_c consumption, the optimal behavior of the network is obtained with small values of P_{max} .

The effect of increasing required rate of IoT devices (R_{min}) on the system EE shown in Fig. 5. It is observed that the total EE decreases with the increasing values of R_{min} . The possible reason for this is the increase in the transmit power to satisfy the required rate of those IoT devices with weaker channel gains. However, this will reduce the overall EE of the network. If the rate requirement can not be satisfied by varying $\Lambda_{i,k}$ then the system increases P_k which results in further decreasing the EE. Data rate of IoT devices is a logarithmic function of power, hence, allocating more power to meet the rate requirement it results in decreasing the EE of the system. This can also be seen from the EE definition in (7), as the numerator increases logarithmically with power and

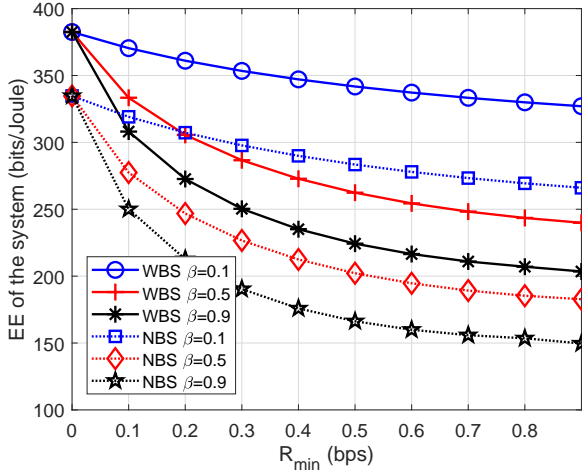


Fig. 5: The impact of increasing R_{min} on the EE with different β

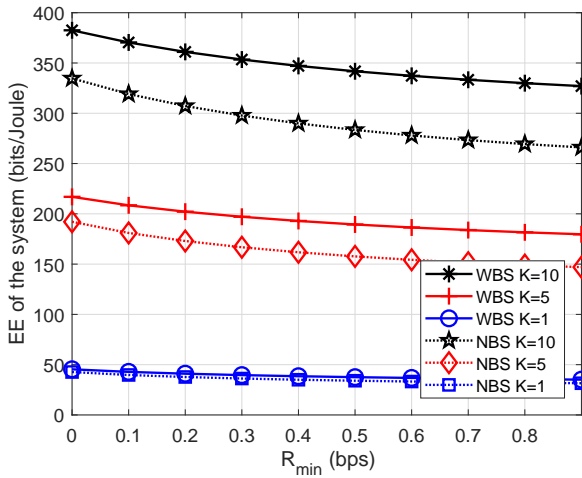


Fig. 6: The effect of increasing R_{min} on the EE with different number of cells

the increase in denominator is linear, when power allocation is increased beyond the optimal point, the EE of the system reduces. Another interesting thing to note in the Fig. 5 is that when R_{min} is increased the EE of NBS decreases more rapidly as compared to WBS. This is because in NBS system when the allocated power is increased, it also results in increasing the interference which further adds to decrease the EE. However, in the case of WBS, allocating more power also enhances the data rate of BST rate, so this compensates for the increased interference to some extent.

The results in Fig. 6 depicts the gap of system EE of WBS and NBS. The performance gap increases with the increase in K . This is because when the number of K is increased, the total BST in the system also increases, so the benefit of BSC becomes more prominent. Another point to note is that in the case of WBS when R_{min} is increased, the reduction in the case of $K=10$ is more rapid as compared to the system with 5 cells, and the network with only one cell faces the least reduction in the EE. This is because the IoT devices in the system having more cells receive more interference. Thus,

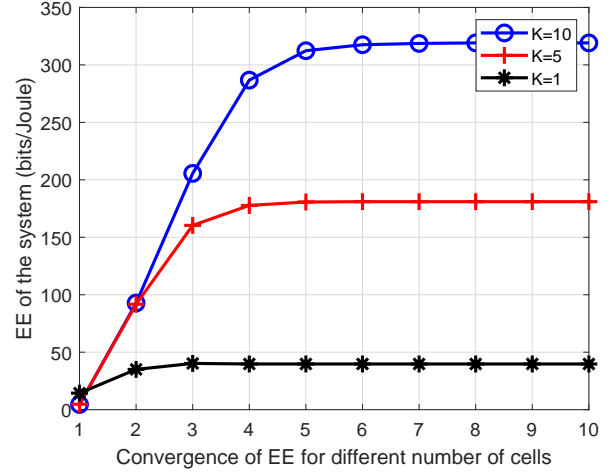


Fig. 7: Convergence of EE for different number of cells

when the allocated power is increased to satisfy the minimum rate requirement, the EE decreases rapidly (for $K=10$ each user faces interference from 9 other cells, whereas in the case of $K=5$, the inter-cell interference is caused by 4 cells). In the case of $K=1$ the users only face intra-cell interference which is somewhat compensated by the BST, hence in this case, the decrease in the EE is minimal.

The convergence behavior of the proposed framework is shown in Fig. 7. When the number of the cells in the system are increased, the number of optimization variables increases which results in increasing the complexity of the system. The Fig. 7 shows that the system with just one cells takes the least number of iterations to converge, whereas the system with 10 cells is the slowest to converge. However, it can be seen that for any number of cells in the system, the proposed framework converges within limited iterations.

V. CONCLUSION

BSC and NOMA are the two emerging technologies to connect large-scale low-powered IoT devices in coming 6G era. In this paper, we has proposed the EE maximization approach for multi-cell NOMA BSC under the assumption of imperfect SIC. In particular, the power of source, PAC of IoT devices and RC of BST in each each have been jointly optimized to maximize total EE of the network. The Dinkelbach's algorithm has adopted first to transform the optimization followed by KKT conditions and dual method to obtain the efficient solutions. The simulation results has shown that the proposed multi-cell NOMA BSC framework outperforms the benchmark optimization framework and converges in a few iterations.

APPENDIX A: PROOF OF PROPOSITION 1

Here, concavity/convexity of R_k w.r.t. $\Phi_{f,k}$ is proved. The first derivative of R_k w.r.t. $\Phi_{f,k}$ is given as:

$$\frac{\partial R_k}{\partial \Phi_{f,k}} = \frac{Y_{i,k}}{\ln(2)(A_{i,k} + Z_{i,k})} + \frac{C_{j,k}}{\ln(2)(B_{j,k}^2 + B_{j,k}A_{j,k})} \quad (38)$$

where $A_{i,k} = (X_{i,k} + \Phi_{f,k}Y_{i,k})$, $A_{j,k} = (X_{j,k} + \Phi_{f,k}Y_{j,k})$, $B_{j,k} = (Z_{j,k} + \Phi_{f,k}W_{j,k})$, and $C_{j,k} = (Y_{j,k}Z_{j,k} - X_{j,k}W_{j,k})$. It's second order derivative is as:

$$\frac{\partial^2 R_k}{\partial \Phi_{f,k}^2} = - \left(\frac{Y_{i,k}^2}{\ln(2)(A_{i,k} + Z_{i,k})^2} + \frac{C_{j,k}(2W_{j,k}E_{j,k} + C_{j,k}^+)}{\ln(2)B_{j,k}^2(B_{j,k} + B_{j,k}A_{j,k})^2} \right) < 0 \quad (39)$$

where $E_{j,k} = B_{j,k} + Y_{j,k}\Phi_{f,k}$, and $C_{j,k}^+ = (Y_{j,k}Z_{j,k} + X_{j,k}W_{j,k})$.

We can see that (39) is negative, therefore R_k is concave/convex and is an increasing function with $\Phi_{f,k}$.

APPENDIX B: PROOF OF PROPOSITION 2

We employ the dual method to obtain an efficient closed-form solution for convex optimization problem in (11) with respect to RC of BST. The Lagrangian function of problem (11) can be defined as:

$$\begin{aligned} L(\Phi_{f,k}, \lambda_{i,k}, \lambda_{j,k}, \mu_k, \eta_{f,k}) &= \sum_{k=1}^K N_k(\Phi_{f,k}) \\ &- \Pi \sum_{k=1}^K P_k(A_{i,k} + A_{j,k}) - p_c + \lambda_{i,k}Q(\Phi_{f,k}, i, k) \\ &+ \lambda_{j,k}Q(\Phi_{f,k}, j, k) + \mu_k(P_{max} - P_k) + \eta_{f,k}R(\Phi_{f,k}) \end{aligned} \quad (40)$$

where

$$\begin{aligned} N_k(\Phi_{f,k}) &= \log_2 \left\{ \left(1 + \frac{X_{i,k} + \Phi_{f,k}Y_{i,k}}{Z_{i,k}} \right) \right. \\ &\left. + \log_2 \left(1 + \frac{X_{j,k} + \Phi_{f,k}Y_{j,k}}{Z_{j,k} + \Phi_{f,k}W_{j,k}} \right) \right\} \end{aligned} \quad (41)$$

$$Q(\Phi_{f,k}, i, k) = X_{i,k} + \Phi_{f,k}Y_{i,k} - (2^{R_{min}} - 1)Z_{i,k} \quad (42)$$

$$\begin{aligned} Q(\Phi_{f,k}, j, k) &= X_{j,k} + \Phi_{f,k}Y_{j,k} - (2^{R_{min}} - 1) \\ &\times (Z_{j,k} + \Phi_{f,k}W_{j,k}) \end{aligned} \quad (43)$$

$$R(\Phi_{f,k}) = \Phi_{f,k} - 1 \quad (44)$$

In (40) $\lambda_{i,k}$, $\lambda_{j,k}$, μ_k and $\eta_{f,k}$ are called the Lagrangian multipliers. Next, we exploit the KKT conditions such as:

$$\frac{\partial L(\Phi_{f,k}, \lambda_{i,k}, \lambda_{j,k}, \mu_k, \eta_{f,k})}{\partial \Phi_{f,k}} \Big|_{\Phi=\Phi^*} = 0, \quad (45)$$

The above equation results in

$$\begin{aligned} \frac{Y_{i,k}}{\ln(2)(A_{i,k} + Z_{i,k})} + \frac{C_{j,k}}{\ln(2)(B_{j,k}^2 + B_{j,k}A_{j,k})} + \lambda_{i,k}Y_{i,k} \\ + \lambda_{j,k}(Y_{j,k} - (2^{R_{min}} - 1)W_{j,k}) + \eta_{f,k} = 0 \end{aligned} \quad (46)$$

$$\begin{aligned} \frac{Y_{i,k}}{\ln(2)(A_{i,k} + Z_{i,k})} + \frac{C_{j,k}}{\ln(2)(B_{j,k}^2 + B_{j,k}A_{j,k})} + \eta_{f,k} \\ = (\lambda_{j,k}(2^{R_{min}} - 1)W_{j,k} - \lambda_{j,k}Y_{j,k}) - \lambda_{i,k}Y_{i,k} \end{aligned} \quad (47)$$

In (46), $C_{j,k} = Y_{j,k}Z_{j,k} - X_{j,k}W_{j,k} = \Delta_{j,k}^k + \sigma^2 > 0$. The left hand side of (46) is always positive and therefore

$$(\lambda_{j,k}(2^{R_{min}} - 1)W_{j,k} - \lambda_{j,k}Y_{j,k}) > \lambda_{i,k}Y_{i,k} \quad (48)$$

In (48), $(\lambda_{j,k}(2^{R_{min}} - 1)W_{j,k} - \lambda_{j,k}Y_{j,k})$ is always positive because $(2^{R_{min}} - 1)$ is always positive and $W_{j,k} > Y_{j,k}$. Since $\lambda_{i,k} \geq 0$, the $\lambda_{j,k}$ is nonnegative. The slack complementary condition in KKT conditions is satisfied. Therefore, $Q(\Phi_{f,k}, i, k)$ and $Q(\Phi_{f,k}, j, k)$ corresponding to $\lambda_{i,k}$ and $\lambda_{j,k}$ are active. Hence, $Q(\Phi_{f,k}, i, k) = 0$ and $Q(\Phi_{f,k}, j, k) = 0$. Finally, the optimum $\Phi_{f,k}$ is obtained from active inequality constraint as given in (13).

APPENDIX C: PROOF OF PROPOSITION 3

Here, the concavity/convexity of $\Lambda_{i,k}$ and $\Lambda_{j,k}$ is proved. The Hessian matrix should be negative definite, if a function is concave. The Hessian matrix is negative definite, when its principal minors have alternative signs. Here we derive a Hessian matrix for our formulated problem and demonstrate it as negative definite. The sum-rate of S_k can be written as:

$$R_k = \log_2(1 + \gamma_{i \rightarrow i}^k) + \log_2(1 + \gamma_{j \rightarrow j}^k) \quad (49)$$

$$\begin{aligned} R_k &= \log_2 \left(1 + \frac{P_k \Lambda_{i,k} \Lambda_{i,k}}{P_k \Lambda_{j,k} B_{i,k} + C_{i,k}} \right) \\ &+ \log_2 \left(1 + \frac{P_k \Lambda_{j,k} \Lambda_{j,k}}{P_k \Lambda_{i,k} B_{j,k} + C_{j,k}} \right) \end{aligned} \quad (50)$$

The Hessian matrix of (50) is defined as:

$$H = \begin{bmatrix} \frac{\partial R_k}{\partial^2 \Lambda_{i,k}} & \frac{\partial R_k}{\partial \Lambda_{i,k} \partial \Lambda_{j,k}} \\ \frac{\partial R_k}{\partial \Lambda_{j,k} \partial \Lambda_{i,k}} & \frac{\partial R_k}{\partial^2 \Lambda_{j,k}} \end{bmatrix} \quad (51)$$

$$\begin{aligned} \frac{\partial R_k}{\partial^2 \Lambda_{i,k}} &= \varphi_{1,1} = - \\ &\frac{A_{i,k}^2 V_{j,k}^2 T_{j,k}^2 - A_{j,k} B_{j,k}^2 T_{i,k}^2 (2V_{j,k} + A_{j,k} \Lambda_{j,k}) \Lambda_{j,k}}{\ln(2) T_{i,k}^2 T_{j,k}^2 V_{j,k}^2} \end{aligned} \quad (52)$$

$$\begin{aligned} \frac{\partial R_k}{\partial \Lambda_{i,k} \partial \Lambda_{j,k}} &= \varphi_{1,2} \\ &= - \frac{A_{i,k} B_{i,k} T_{j,k}^2 - A_{j,k} B_{j,k} T_{i,k}^2}{\ln(2) T_{i,k}^2 T_{j,k}^2} \end{aligned} \quad (53)$$

$$\begin{aligned} \frac{\partial R_k}{\partial^2 \Lambda_{j,k}} &= \varphi_{2,1} \\ &= - \frac{A_{j,k}^2 V_{i,k}^2 T_{i,k}^2 - A_{i,k} B_{i,k}^2 T_{j,k}^2 (2V_{i,k} + A_{i,k} \Lambda_{i,k}) \Lambda_{i,k}}{\ln(2) T_{j,k}^2 T_{i,k}^2 V_{i,k}^2} \end{aligned} \quad (54)$$

$$\begin{aligned} \frac{\partial R_k}{\partial \Lambda_{j,k} \partial \Lambda_{i,k}} &= \varphi_{2,2} \\ &= - \frac{A_{i,k} B_{i,k} T_{j,k}^2 - A_{j,k} B_{j,k} T_{i,k}^2}{\ln(2) T_{i,k}^2 T_{j,k}^2} \end{aligned} \quad (55)$$

where, $T_{i,k} = A_{i,k} \Lambda_{i,k} + V_{i,k}$, $T_{j,k} = A_{j,k} \Lambda_{j,k} + V_{j,k}$, $V_{i,k} = B_{i,k} \Lambda_{j,k} + C_{i,k}$, and $V_{j,k} = B_{j,k} \Lambda_{i,k} + C_{j,k}$. The obtained

Hessian matrix can be expressed as:

$$H = \begin{bmatrix} \varphi_{1,1} & \varphi_{1,2} \\ \varphi_{2,1} & \varphi_{2,2} \end{bmatrix} \quad (56)$$

We can see that $\varphi_{1,1}$ and $\varphi_{2,2}$ in (56) are the first order principle minors and also negative. Moreover, it can be evident that the second order minors are the determinant of (56) and can be written as

$$\det H = \varphi_{1,1}\varphi_{2,2} - \varphi_{1,2}\varphi_{2,1} > 0 \quad (57)$$

APPENDIX D: PROOF OF PROPOSITION 4

The derivative of Equation 19 with respect to $A_{i,k}$ is

$$\begin{aligned} \frac{\partial L(\mathbf{A}_k, \boldsymbol{\lambda}_k, \boldsymbol{\mu}_k, \epsilon_k)}{\partial A_{i,k}} &= \frac{A_{i,k}}{\ln(2)(A_{i,k}A_{i,k} + B_{i,k}A_{j,k} + C_{i,k})} \\ &+ \frac{A_{j,k}B_{j,k}A_{j,k}}{\ln(2)(B_{j,k}A_{i,k} + C_{j,k})(A_{j,k} - A_{j,k} + B_{j,k}A_{i,k} + C_{j,k})} \\ &- D \end{aligned} \quad (58)$$

where $D = \Pi P_k - \lambda_{i,k}A_{i,k} + \lambda_{j,k}(2^{R_{min}} - 1)B_{j,k} + \epsilon_k$. Put $A_{j,k} = 1 - A_{i,k}$ in Equation (34) which results in

$$\frac{A_{i,k}}{\ln(2)(X_{i,k}A_{i,k} + W_{i,k})} - \frac{\gamma_{j \rightarrow j}^k B_{j,k}}{\ln(2)(Y_{j,k}A_{i,k} + W_{j,k})} - D \quad (59)$$

where $X_{i,k} = A_{i,k} - B_{i,k}$, $Y_{j,k} = B_{j,k} - A_{j,k}$, $W_{i,k} = B_{i,k} + C_{i,k}$ and $W_{j,k} = A_{j,k} + C_{j,k}$.

After some manipulation, Equation (35) results as:

$$\begin{aligned} A_{i,k}(Y_{j,k}A_{i,k} + W_{j,k}) - \gamma_{j \rightarrow j}^k B_{j,k}(X_{i,k}A_{i,k} + W_{i,k}) \\ - \ln(2)D(Y_{j,k}A_{i,k} + W_{j,k})(X_{i,k}A_{i,k} + W_{i,k}) = 0 \end{aligned} \quad (60)$$

After expanding and writing in $ax^2 + bx + c$

$$\begin{aligned} (-\ln(2)DX_{i,k}Y_{j,k})A_{i,k}^2 + (A_{i,k}Y_{j,k} - \gamma_{j \rightarrow j}^k B_{j,k}X_{i,k} \\ - \ln(2)DX_{i,k}W_{j,k} - \ln(2)DY_{j,k}W_{i,k})A_{i,k} + (A_{i,k}W_{j,k} \\ - \gamma_{j \rightarrow j}^k B_{j,k}W_{i,k} - \ln(2)DW_{i,k}W_{j,k}) \end{aligned} \quad (61)$$

The solution of above problem is as follow,

$$A_{i,k} = \left[\frac{-b \pm \sqrt{b^2 - 4ac}}{2a} \right]^+ \quad (62)$$

The proof is completed.

REFERENCES

- [1] F. Jameel *et al.*, "NOMA-enabled backscatter communications: Toward battery-free IoT networks," *IEEE Internet of Things Magazine*, vol. 3, no. 4, pp. 95–101, Dec. 2020.
- [2] W. Liu *et al.*, "Next generation backscatter communication: systems, techniques, and applications," *EURASIP J. Wireless Commun. Netw.*, vol. 2019, no. 1, pp. 1–11, 2019.
- [3] W. U. Khan *et al.*, "NOMA-enabled optimization framework for next-generation small-cell IoV networks under imperfect SIC decoding," *IEEE Transactions on Intelligent Transportation Systems*, pp. 1–10, 2021.
- [4] A. U. Khan *et al.*, "An enhanced spectrum reservation framework for heterogeneous users in CR-enabled IoT networks," *IEEE Wireless Communications Letters*, pp. 1–1, 2021.
- [5] A. U. Khan *et al.*, "Spectrum utilization efficiency in CRNs with hybrid spectrum access and channel reservation: A comprehensive analysis under prioritized traffic," *Future Generation Computer Systems*, vol. 125, pp. 726–742, 2021.
- [6] F. Jameel *et al.*, "Applications of backscatter communications for healthcare networks," *IEEE Network*, vol. 33, no. 6, pp. 50–57, Nov–Dec. 2019.
- [7] W. U. Khan *et al.*, "Joint spectral and energy efficiency optimization for downlink NOMA networks," *IEEE Trans. Cogn. Commun. Netw.*, vol. 6, no. 2, pp. 645–656, June 2020.
- [8] X. Lu *et al.*, "Ambient backscatter assisted wireless powered communications," *IEEE Wireless Communications*, vol. 25, no. 2, pp. 170–177, Apr. 2018.
- [9] W. U. Khan *et al.*, "Energy-efficient resource allocation for 6G backscatter-enabled NOMA IoV networks," *IEEE Transactions on Intelligent Transportation Systems*, pp. 1–11, 2021.
- [10] A. Ihsan *et al.*, "Energy-efficient backscatter aided uplink NOMA roadside sensor communications under channel estimation errors," *arXiv preprint arXiv:2109.05341*, 2021.
- [11] N. Van Huynh *et al.*, "Ambient backscatter communications: A contemporary survey," *IEEE Commun. Surveys Tutor.*, vol. 20, no. 4, pp. 2889–2922, Fourthquarter 2018.
- [12] O. Maraqa *et al.*, "A survey of rate-optimal power domain NOMA with enabling technologies of future wireless networks," *IEEE Commun. Surveys Tutor.*, vol. 22, no. 4, pp. 2192–2235, 2020.
- [13] W. U. Khan *et al.*, "Joint spectrum and energy optimization of NOMA-enabled small-cell networks with QoS guarantee," *IEEE Transactions on Vehicular Technology*, vol. 70, no. 8, pp. 8337–8342, Aug. 2021.
- [14] Z. Ding *et al.*, "Application of non-orthogonal multiple access in LTE and 5G networks," *IEEE Commun. Mag.*, vol. 55, no. 2, pp. 185–191, Feb 2017.
- [15] Z. Ali *et al.*, "Fair power allocation in cooperative cognitive systems under NOMA transmission for future IoT networks," *Alexandria Engineering Journal*, vol. 61, no. 1, pp. 575–583, 2022.
- [16] H. Guo *et al.*, "Cooperative ambient backscatter system: A symbiotic radio paradigm for passive IoT," *IEEE Wireless Commun. Lett.*, vol. 8, no. 4, pp. 1191–1194, Aug. 2019.
- [17] Y. Ye *et al.*, "On the outage performance of ambient backscatter communications," *IEEE IoT J.*, vol. 7, no. 8, pp. 7265–7278, Aug. 2020.
- [18] F. Jameel *et al.*, "Simultaneous harvest-and-transmit ambient backscatter communications under Rayleigh fading," *EURASIP J. Wireless Commun. Net.*, vol. 2019, no. 1, pp. 1–9, Dec. 2019.
- [19] J. Qian *et al.*, "IoT communications with M -PSK modulated ambient backscatter: Algorithm, analysis, and implementation," *IEEE IoT J.*, vol. 6, no. 1, pp. 844–855, Feb. 2019.
- [20] B. Lyu *et al.*, "The optimal control policy for RF-powered backscatter communication networks," *IEEE Trans. Vehicular Techn.*, vol. 67, no. 3, pp. 2804–2808, Mar. 2018.
- [21] F. Jameel *et al.*, "Low latency ambient backscatter communications with deep Q-learning for beyond 5G applications," in *IEEE VTC2020-Spring*, 2020, pp. 1–6.
- [22] X. Li *et al.*, "Physical layer security of cognitive ambient backscatter communications for green internet-of-things," *IEEE Trans. Green Commun. Netw.*, pp. 1–1, 2021.
- [23] F. Jameel *et al.*, "Towards intelligent IoT networks: Reinforcement learning for reliable backscatter communications," in *2019 IEEE Globecom Workshops (GC Wkshps)*, 2019, pp. 1–6.
- [24] —, "Reinforcement learning for scalable and reliable power allocation in SDN-based backscatter heterogeneous network," in *IEEE INFOCOM 2020 - IEEE Conference on Computer Communications Workshops (INFOCOM WKSHPS)*, 2020, pp. 1069–1074.
- [25] C.-B. Le and D.-T. Do, "Outage performance of backscatter NOMA relaying systems equipping with multiple antennas," *Electronics Letters*, vol. 55, no. 19, pp. 1066–1067, Sept. 2019.
- [26] Q. Zhang *et al.*, "Backscatter-NOMA: A symbiotic system of cellular and internet-of-things networks," *IEEE Access*, vol. 7, pp. 20000–20013, 2019.
- [27] X. Li *et al.*, "Secrecy analysis of ambient backscatter NOMA systems under IQ imbalance," *IEEE Trans. Veh. Technol.*, vol. 69, no. 10, pp. 12 286–12 290, Oct. 2020.
- [28] W. U. Khan *et al.*, "Backscatter-enabled efficient V2X communication with non-orthogonal multiple access," *IEEE Trans. Veh. Technol.*, vol. 70, no. 2, pp. 1724–1735, Feb. 2021.
- [29] Y. Liao *et al.*, "Resource allocation in NOMA-enhanced full-duplex symbiotic radio networks," *IEEE Access*, vol. 8, pp. 22 709–22 720, 2020.
- [30] J. Guo *et al.*, "Design of non-orthogonal multiple access enhanced backscatter communication," *IEEE Trans. Wireless Commun.*, vol. 17, no. 10, pp. 6837–6852, Oct. 2018.

- [31] A. Farajzadeh *et al.*, "UAV data collection over NOMA backscatter networks: UAV altitude and trajectory optimization," in *IEEE ICC 2019*, 2019, pp. 1–7.
- [32] G. Yang *et al.*, "Resource allocation in NOMA-enhanced backscatter communication networks for wireless powered IoT," *IEEE Wireless Commun. Lett.*, vol. 9, no. 1, pp. 117–120, Jan. 2020.
- [33] S. Zeb *et al.*, "NOMA enhanced backscatter communication for green IoT networks," in *IEEE 16th International Symposium on Wireless Communication Systems (ISWCS)*, 2019, pp. 640–644.
- [34] Y. Li *et al.*, "Secure beamforming in MISO NOMA backscatter device aided symbiotic radio networks," *arXiv preprint arXiv:1906.03410*, 2019.
- [35] Y. Xu *et al.*, "Energy efficiency maximization in NOMA enabled backscatter communications with QoS guarantee," *IEEE Wireless Commun. Lett.*, vol. 10, no. 2, pp. 353–357, Feb. 2021.
- [36] X. Li *et al.*, "Hardware impaired ambient backscatter NOMA systems: Reliability and security," *IEEE Trans. Commun.*, pp. 1–1, 2021.
- [37] W. U. Khan *et al.*, "Backscatter-enabled NOMA for future 6G systems: A new optimization framework under imperfect SIC," *IEEE Commun. Lett.*, pp. 1–1, 2021.
- [38] X. Li *et al.*, "Cooperative wireless-powered NOMA relaying for B5G IoT networks with hardware impairments and channel estimation errors," *IEEE Internet Things J.*, pp. 1–1, 2020.
- [39] W. U. Khan *et al.*, "Spectral efficiency optimization for next generation NOMA-enabled IoT networks," *IEEE Trans. Veh. Technol.*, vol. 69, no. 12, pp. 15 284–15 297, Dec. 2020.
- [40] M. R. Zamani *et al.*, "Energy-efficient power allocation for NOMA with imperfect CSI," *IEEE Trans. Veh. Technol.*, vol. 68, no. 1, pp. 1009–1013, Jan. 2019.
- [41] F. Jameel *et al.*, "Efficient power-splitting and resource allocation for cellular V2X communications," *IEEE Transactions on Intelligent Transportation Systems*, vol. 22, no. 6, pp. 3547–3556, June 2021.